CHEMISTRY
A EUROPEAN JOURNAL

ChemPubSoc
Europe

DOI: 10.1002/chem.201204343

Molecular Design Principle of All-organic Dyes for Dye-Sensitized Solar Cells

Bong-Gi Kim,[a] Kyeongwoon Chung,[b] and Jinsang Kim*[a, b, c]

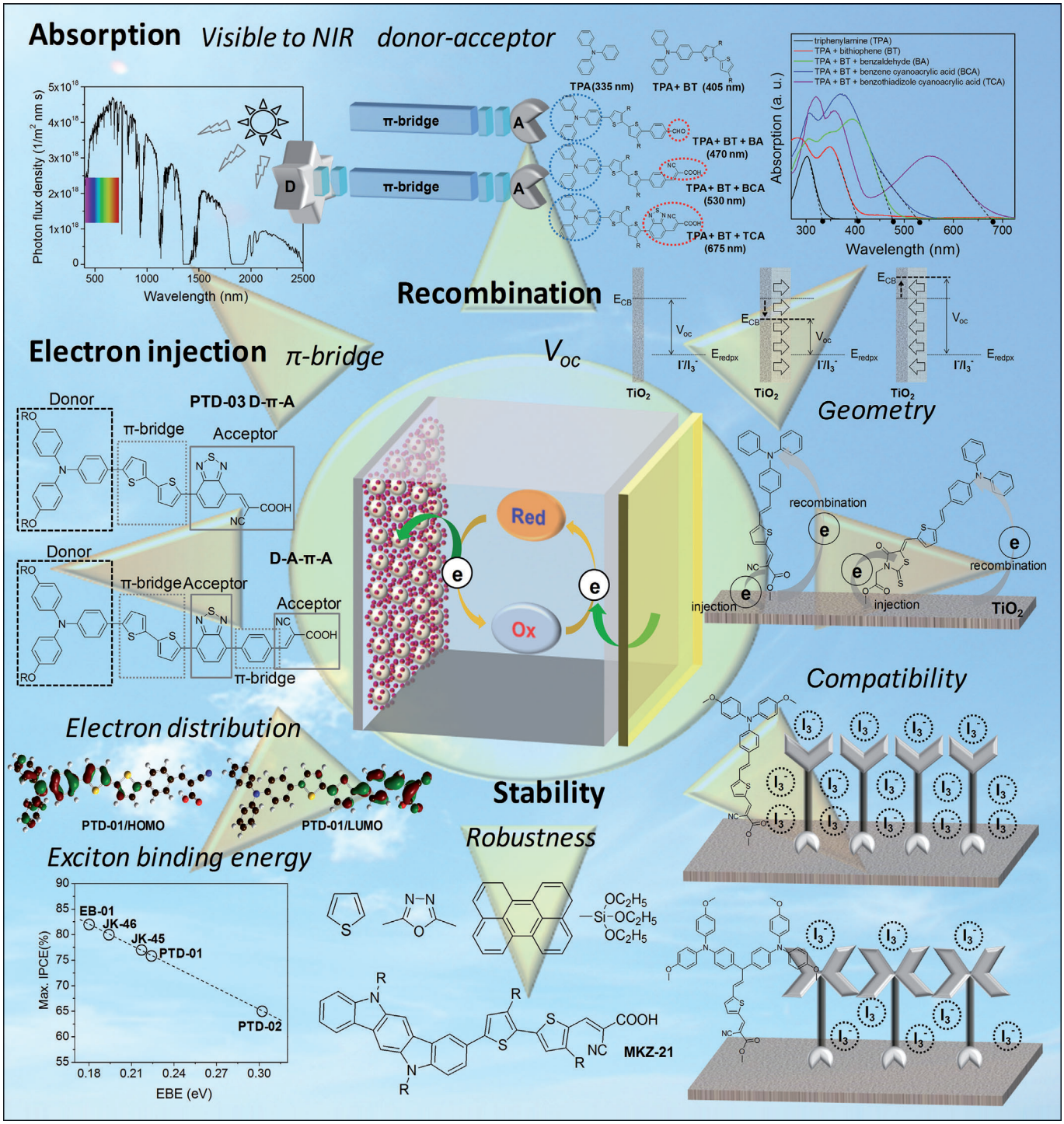

Abstract: All-organic dyes have shown promising potential as an effective sensitizer in dye-sensitized solar cells (DSSCs). The design concept of all-organic dyes to improve light-to-electric-energy conversion is discussed based on the absorption, electron injection, dye regeneration, and recombination. How the electron-donor–acceptor-type framework can provide better light harvesting through bandgap-tuning and why proper arrangement of acceptor/anchoring groups within a conjugated dye frame is important in suppressing improper charge recombination in DSSCs are discussed. Separating the electron acceptor from the anchoring unit in the donor–acceptor-type organic dye would be a promising strategy to reduce recombination and improve photocurrent generation.

Keywords: all-organic dyes · dyses/pigments · dye sensitized solar cells · energy conversion · sensitizers · synthesis design

Introduction

In recent years, dye-sensitized solar cells (DSSCs) have received significant attention as potential alternatives to conventional silicon-based solar cells, owing to their cost effectiveness and relatively high energy conversion efficiency.[1–9] The overall power conversion efficiency has improved rapidly, with values over 12% when liquid electrolyte is adopted,[10–12] and long-term stability for the practical application has been achieved.[13] In general, the sensitizing dye is anchored to a wide-bandgap semiconducting oxide, such as TiO_2, ZnO, and SnO_2 in DSSCs and acts as an agent to convert solar-light to electric power. As illustrated in Figure 1, photocurrent is generated through light absorption, electron injection, and dye regeneration, and the open-circuit voltage (V_{oc}) is determined from the theoretical potential-energy difference between the semiconducting oxide and the applied electrolyte after considering the degree of recombination. The sensitizing dye partakes in all three of the photocurrent generation steps as well as the determination of V_{oc}. The degree of light absorption originates from the dye's optical band-gap, the driving force for the electron injection from

[a] Dr. B.-G. Kim, Prof. J. Kim
Department of Material Science and Engineering
University of Michigan, Ann Arbor, Michigan 48109 (USA)
Fax: (+1) 734-763-4788
E-mail: jinsang@umich.edu
[b] K. Chung, Prof. J. Kim
Macromolecular Science and Engineering
University of Michigan, Ann Arbor, Michigan 48109 (USA)
[c] Prof. J. Kim
Department of Chemical Engineering
University of Michigan, Ann Arbor, Michigan 48109 (USA)

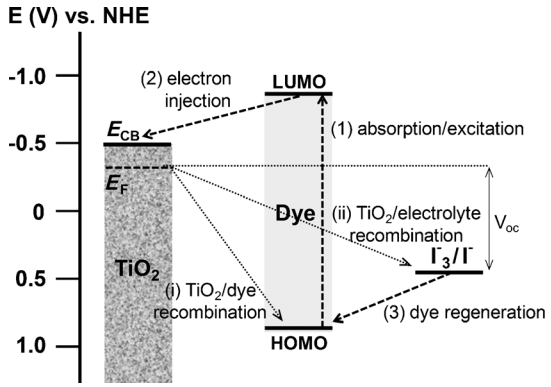

Figure 1. Device operation in DSSCs and required relative energy level of each component.

dye's lowest unoccupied molecular orbital (LUMO) to semiconducting oxide's conduction band (E_{CB}) depends on their potential-energy difference, and oxidized dye's regeneration rate or the degree of recombination is related with structural change of organic dyes.[14] Thus, photosensitizing dyes critically affect the solar-to-electric-power conversion efficiency of DSSCs.

Since Grätzel and O'Regan reported an efficient DSSC system with polypyridyl ruthenium(II) complex dyes adsorbed on a nanocrystalline n-type semiconductor TiO_2 electrode in 1991,[1] various types of dyes have been explored to improve overall device performance. All of them, however, satisfied the following common factors to efficiently convert solar-light to electric power. First, they have at least one anchoring group that chemically binds dyes onto the semiconducting oxide surface. As an example, a carboxyl group, one of most common anchoring groups for sensitizing dyes in DSSCs, makes a unidentate ester, a bidentate-chelating, or a bidentate-bridging linkage with the TiO_2 surface, providing a strongly bound dye leading to better electronic coupling with the TiO_2.[15] Second, the dye's LUMO level must be higher than the E_{CB} of the applied semiconducting electrode for efficient electron injection from the dye to the electrode, and the dye's highest occupied molecular orbital (HOMO) level must be lower than the redox potential of the applied electrolyte for efficient dye regeneration from its oxidized state. Third, the absorption region of dyes should match with the solar spectrum, especially the highest photon-flux region in order to harvest as much light as possible. Fourth, dye aggregation should be avoided, because it reduces electron-injection efficiency from the dye to the semiconducting oxide through intermolecular energy transfer, resulting in low solar-to-electric-energy conversion efficiency.[16,17] Finally, dyes should be chemically stable throughout the photocurrent generation cycle.

Metal complexes, typically ruthenium (Ru), have drawn much interest as a promising candidate due to their broad absorption through metal-to-ligand charge transfer (MLCT), the longer exciton lifetime, and their long-term chemical sta-

bility.[3] However, the limited availability of Ru as a noble metal hampers its wide application potential, which has led to the rapid development of all-organic dyes. Compared to the metal complexes, all-organic dyes have several advantageous features, such as lower material costs, elimination of environmental issues, larger molar extinction coefficient, and infinite flexibility in molecular design.[18–20] Various all-organic dyes containing triphenylamine, coumarin, merocyanine, indoline, fluorene, or carbazole moieties[18,21–32] have been explored intensively, and the energy conversion efficiency of DSSCs employing all-organic dyes has rapidly improved to up to over 9.0%.[18,28,33,34] However, for all-organic dyes to be an efficient sensitizer for practical application, they have to overcome several disadvantages, such as shorter exciton lifetimes in their excited states, when compared to metal complexes, the tendency to aggregate, and a relatively narrow absorption in the visible region.[20,35,36] In this contribution, we introduce molecular design concepts of all-organic dyes in order to additionally improve their solar-to-electrical-energy conversion efficiency in DSSCs. Discussions are described in the order of absorption, electron injection, dye regeneration, recombination, and stability.

Dye Design Regarding Absorption

The fundamental requirement for photovoltaic energy conversion is the collection of as much sunlight as possible. However, the main absorption ranges of typical all-organic dyes are limited within 200 nm, because it is determined by the molecular orbital hybridization through a conjugated dye frame. As shown in Figure 2a, the photon flux density, which indicates the number of photons that can excite ground-state electrons with corresponding energy at the wavelength, has a conspicuous distribution, and the highest photon flux region stands around 600 to 800 nm. For example, if a dye can completely absorbs solar radiation from 280 to 500 nm it can theoretically produce 5.1 mA cm^{-2} as illustrated in Figure 2b, but this current density is even smaller than the expected current density (6.5 mA cm^{-2} = 11.1–17.6 in Fig 2b) of a dye which can cover only from 600 to 700 nm, because of the unique distribution of the photon flux density of solar radiation. In this regard, the dye's absorption range should match the high photon flux region of the solar spectrum, thus the ability to tailor the optical band-gap of dyes for DSSC application is crucially important for efficient solar-light harvesting.

One of the common tools to tailor the absorption of all-organic dyes is the extension of the effective conjugation length, because the absorption band of π-conjugated materials originates from the degree of interaction between π orbitals. However, the degree of π-orbital interaction is also strongly affected by chain conformation, which limits the practical implication of the conjugation length in tuning the absorption range of dyes. Another efficient way to control a dye's absorption range is by combining an electron-donating (donor, D) and an electron-accepting (acceptor, A) moiety

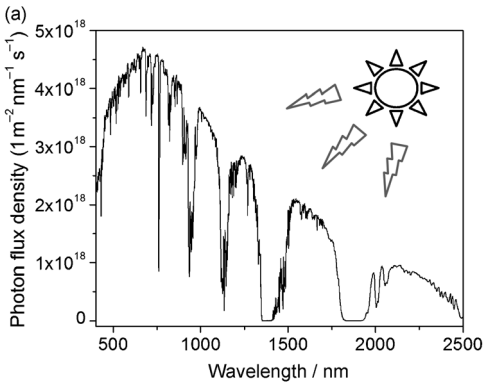

(b)

Wavelength (nm)	Max. % harvested (from 280nm)	Expecting current density (mA cm^{-2})
500	8.0	5.1
600	17.3	11.1
650	22.4	14.3
700	27.6	17.6
750	35.6	20.8
800	37.3	23.8
900	46.7	29.8
1000	53.0	33.9
1250	68.7	43.9
1500	75.0	47.9

Figure 2. a) Photon-flux density of solar radiation. b) Degree of solar-light harvesting and expecting maximum photocurrent density from the harvest.

within the same conjugated framework. The D–A structure induces intramolecular charge transfer (ICT), which facilitates π-orbital overlap via the quinoid resonance structure and produces consequent redshift absorption of the dye.[37] As a representative example to demonstrate the effect of the conjugation length or the D–A framework on dye's absorption, UV/Vis absorption spectra of all-organic dyes with various conjugated units were investigated. In Figure 3, the dashed and solid circles on the chemical structure of such dyes indicate electron-donating and -accepting moieties, respectively. The absorption edge corresponding to the optical band-gap of triphenylamine (TPA) stands around 335 nm, and redshifts to 405 nm when TPA is conjugated with a bithiophene (BT) moiety due to the extended conjugation length (additional 12π electrons). When benzaldehyde (BA) is combined to the TPA+BT molecule, the band edge moves further to 470 nm. In this case, although only additional 6π electrons of the phenyl are added to the TPA+BT molecule, the degree of absorption redshift in the resulting TPA+BT+BA is comparable with the 12π electrons of bithiophene (70 nm); this large shift is likely owing to the fact that the electron-accepting aldehyde moiety improves chain planarity by forming ICT with the electron-donating TPA through the conjugated frame. As electron-accepting capacity increases by replacing the benzaldehyde with benzene cyanoacrylic acid (BCA) or benzothiadiazole cyanoacrylic acid (TCA), the absorption band additionally moves to 530 and finally to 675 nm, respectively. This demonstrates that a dye's absorption can be efficiently tuned by manipulating the degree of electron-donating and -accepting units

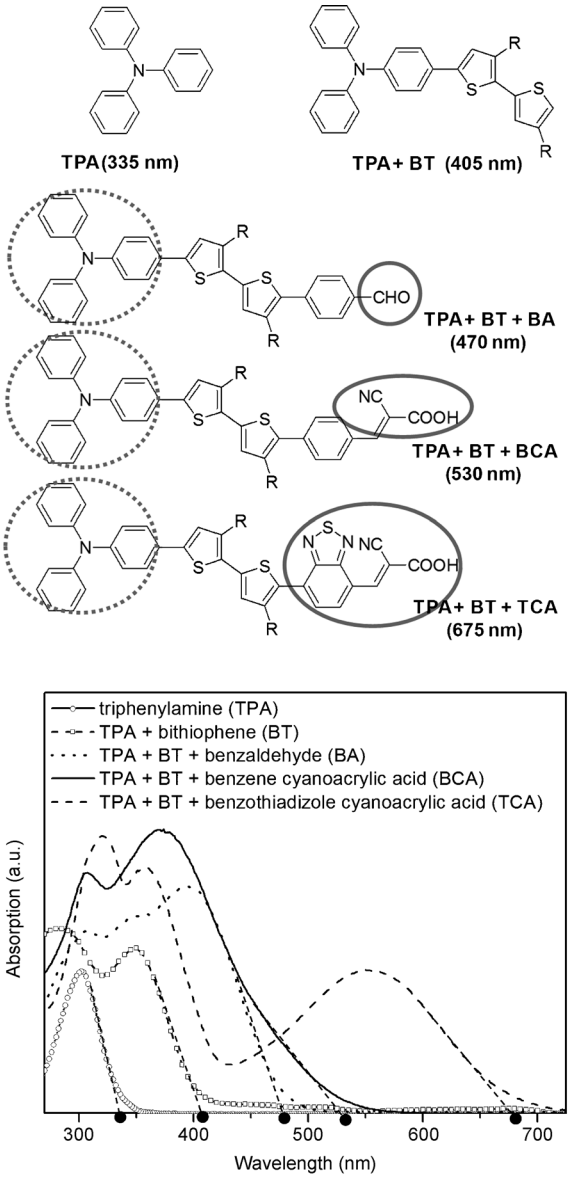

Figure 3. Degree of absorption shift from conjugation length and intramolecular charge transfer.

within a short conjugation length of the D–A framework. Thus, implementing electron donors and acceptors together in a conjugated framework is an effective strategy to modulate absorption band of all-organic dyes.

Most D–A-type all-organic dyes investigated for DSSC application share a common structure. As shown in Figure 4a, D–A organic dyes exhibiting excellent solar-light-harvesting efficiency consist of electron-donating and -accepting moieties at their chain ends, and they are connected through a conjugated π bridge. Diverse electron-donating groups are adopted for all-organic dyes to be applied for DSSCs. Several representative examples, such as carbazole, phenothiazine, triarylamine, coumarin, indoline, tetrahydroquinoline, and triphenylamine, are shown in Figure 4b.[2,21,29,38–40] In addition to an electron-donating effect in all-organic dyes, the electron-donor moiety should be configured such that the dye should not be interpenetrated with adjacent dyes to suppress dye aggregation on the semiconducting oxide surface, because such aggregation induces intermolecular charge transfer and hampers electron injection from dye to the electrode. Basically, the acceptor should have enough capability to withdraw electrons from the donor in all-organic dyes. Essentially, the anchoring units inevitably required to attach dyes on the oxide surface are inherent acceptors and simultaneously act as electron-withdrawing moieties in all-organic dyes. Several standard acceptors, such as carboxylic acid, phosphonic acid, cyanoacrylic acid, rhodanine acetic acid, and benzothiadiazolyl cyanoacrylic acid, are shown in Figure 4d. Cyanoacrylic acid is most commonly employed as an acceptor in D–A dyes, because of its easy synthesis and relatively good stability as an anchoring unit.[41] The role of the π bridge in D–A dyes is to extend the absorption range of the dyes to the visible region. Some representative examples are summarized in Figure 4c. Since the π bridge is the channel through which electrons move from donor to acceptor moieties, it should have a (quasi)planar geometry for efficient electron transfer. However, the planar geometry tends to induce interchain aggregation of the dyes on the semiconducting oxide surface, resulting in the decrease of electron-injection yield. Thus, the π bridge should be selected carefully after considering propensity of aggregation.

Although the D–A structure of all-organic dyes has the advantage of modulating the absorption range, their poor light-to-electric-energy conversion efficiency has limited their wide application for DSSCs. When a strong electron-withdrawing group is located at the proximity of the anchoring moiety, as exemplified with benzo[*c*]-1,2,5-thiadiazole in Figure 5a, the electron-injection efficiency into TiO_2 from the excited dye was critically damaged, because of the charge entrapment effect around the withdrawing group or the strong recombination.[33,42,43] To overcome these drawbacks while preserving the merit of easy absorption modulation, an additional π-bridge (D–π–A–π–A) was recently introduced between the electron-withdrawing and anchoring groups.[43–46] As shown in Figure 5b, the insertion of an additional phenyl ring dramatically improved the light-to-electric-energy conversion efficiency. The incident photon-to-current conversion efficiency (IPCE) was enhanced from 20 to over 90% at their maximum absorption region with subtle absorption blueshift, leading to over 6.5 times higher power conversion efficiency (PCE. 8.21%). Although there was no significant difference in the electron-injection efficiency when the phenyl ring was added, the reduction behavior of the oxidized dye on TiO_2 in the absence of electrolyte was noticeably retarded, indicating slow recombination. Photophysical investigations, such as nanosecond laser photolysis and ultrafast transient absorption measurements, revealed that the insertion of the phenyl ring prevents the back-electron transfer of the charge-separated state, resulting in slow recombination between TiO_2 and dye (vide infra).

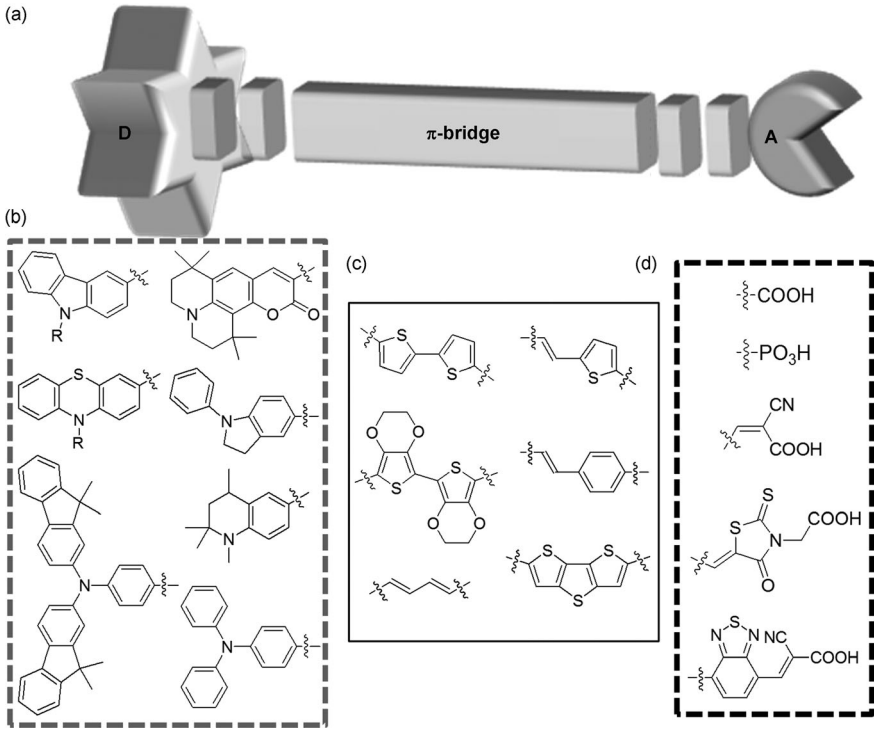

Figure 4. a) Schematic illustration of D–A-type organic dye and representative examples of b) donor, c) π bridge, and d) acceptor.

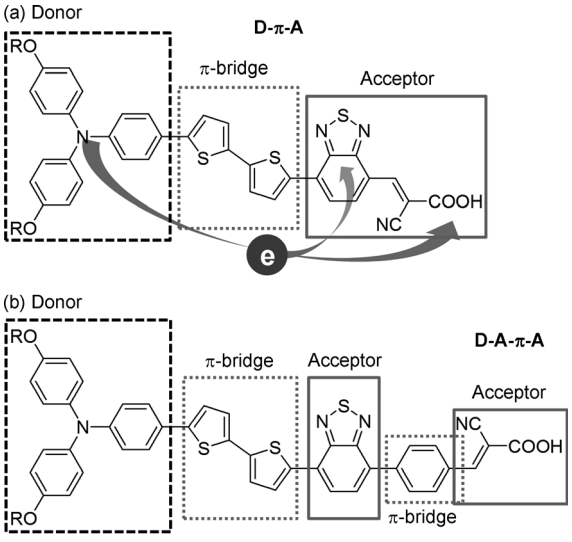

Figure 5. Representative examples of a) D–A-type dye resulting in electron entrapment and b) modified D–A-π-A type organic dye.

Dye Design Regarding Electron Injection

The driving force for the electron injection from a dye to a semiconducting oxide is the energy-level difference between the dye's LUMO level and the E_{CB} of the semiconducting oxides. Thus, fine-tuning of the dye's energy levels by modifying its molecular structure is essential in order to provide an equilibrium in the dye's oxidation/reduction system for efficient charge transfer in DSSCs. However, explaining the electron-injection efficiency only with the dye's required energy levels is not enough, because the degree of electron injection is also strongly affected by the molecular orientation and spatial arrangement of dyes, such as aggregation, and electronic coupling with the electrode.

In all-organic dyes, expansion of π conjugation tends to cause π-stacked aggregation through the formation of intermolecular π–π interactions between dye molecules; these interactions hamper electron injection into the electrode. Dye aggregation on the surface of TiO_2 causes absorption shift to the red (J-aggregation) or blue (H-aggregation) regions relative to the absorption of the monomeric dye. Particularly, H-aggregation usually quenches the excited state and consequently depletes the absorbed light energy without electron injection.[47] The aggregation-dependent, unfavorable light harvesting of all-organic dyes can be easily traced by applying co-adsorption of chenodeoxycholic acid (DCA) with dyes on the TiO_2 surface.[48] The co-adsorbed DCA makes interdye distance larger, reduces intermolecular aggregation, and thereby improves photocurrent generation behavior. In this respect, introduction of a sterically hindered group, such as a bulky side chain and starburst triarylamine, on the periphery of the donor part and/or on a π-conjugated bridge is one of common design strategies to suppress dye aggregation. Although the introduction of sterically hindered substituents to all-organic dyes may diminish the dye's loading density on the TiO_2 surface due to the enlarged molecule size, those dyes normally provide higher photocurrent in DSSCs, when compared to rod-shaped dyes showing strong aggregation accompanied with high loading density.[49] The aggregation tendency of all-organic dyes could be overcome by this simple structural modification. As shown in Figure 6, a simple modification of side chains attached to the same aromatic rigid dye frame results in totally different aggregation behavior and consequent DSSC performance. Relatively bulky benzyl (OH-9) or 5-nonyl (H-10) side chains efficiently suppresses dye aggregation, resulting in the strong emission of the dye in the solid state and renders equivalent photocurrent generation from the absorbed photons.

Organic dye's intrinsic properties, such as shape, geometry, and conjugation length, should also be considered in the dye design to improve electron-injection efficiency. As

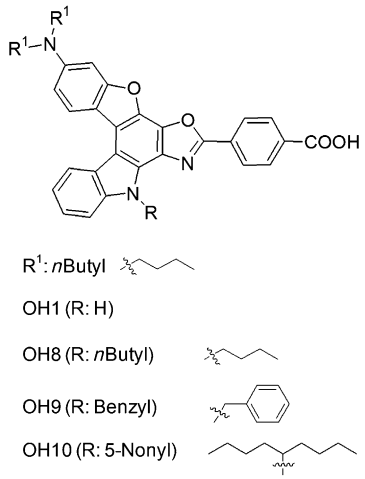

Figure 6. The effect of side chains on dye's aggregation.

shown in Figure 7a, in the HOMO state the electron density of a D–A-type dye is mostly localized around the electron-donating triphenylamine group. However, in the LUMO state the electrons are localized near the electron-withdrawing acceptor (cyanoacetic acid). This indicates that electron should move from donor to acceptor after the light absorption through excitation, and the asymmetric D–A structure is advantageous to direct intramolecular electron transfer from donor to acceptor. For instance, asymmetric squaraine dyes have exhibited much higher photocurrent than analogous symmetrical squaraine dyes, because of the unidirectional flow of electrons.[50]

Another important factor affecting the electron-injection efficiency is the exciton binding energy (EBE) of all-organic dyes. Since DSSCs are excitonic solar cells, the generated photocurrent is inextricably related to the charge dissociation energy, which is quantitatively proportional to the EBE of applied dyes. The EBE is affected by the geometry of the conjugated molecule. Normally the EBE decreases as the conjugation extends.[51] Recently, EBEs of several all-organic dyes sharing a similar chemical nature have been calculated by quantum mechanics methods, and the relationship between the EBE and the maximum incident photon-to-current conversion efficiency (IPCE) of each dye has been correlated.[33] The IPCE represents the degree of energy conversion of an incident photon to current through the dissociation of a bound hole/electron pair (exciton), and therefore the IPCE value reflects dye's absorption efficiency, its quantum yield (QY), and the charge-collection efficiency all together. Thus, as far as experimental conditions satisfy saturated dye absorption and essentially similar charge-collection efficiency by means of the same device architecture, the maximum IPCE value could be directly related to the QY of the applied organic dye. As shown in Figure 7b, the maximum IPCE exhibits a descending linear correlation with the EBEs of the applied dyes, indicating that a dye having a lower EBE will provide a better energy conversion efficiency for DSSC applications.

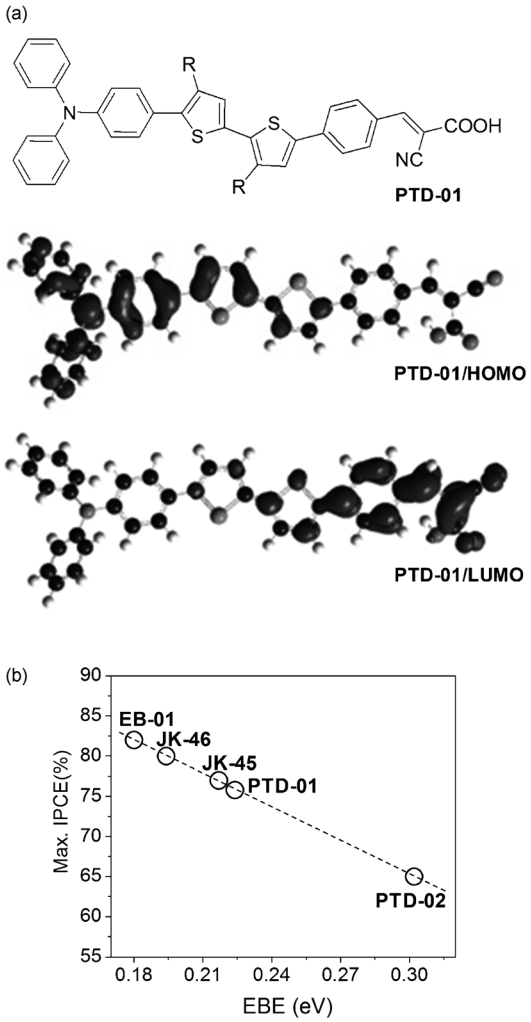

Figure 7. a) Electron distribution of a D–A-type organic dye both in HOMO and LUMO state. b) The correlation between EBE and maximum IPCE.

The formation of good electronic coupling between the LUMO of the dye and the E_{CB} of a semiconducting oxide electrode is also an essential requirement for efficient electron injection. According to the Marcus electron-transfer model, the electron-hopping rate (k_{et}) is quadratically proportional to the electronic coupling (V^2).[52] The electronic coupling is strongly affected by the chemical structure of all-organic dyes, such as the applied anchoring groups of the dye and the electron-withdrawing moiety placed around the anchoring groups. For example, because of its stronger electron-withdrawing ability, rhodanine acetic acid provides a worse light-to-electric-energy conversion efficiency than cyanoacrylic acid, even though rhodanine acetic acid produces better photon-flux absorption.[53] The calculation of dyes' molecular configurations and additional optimization by means of the density functional theory (DFT) has disclosed that in the LUMO state the rhodanine group noticeably reduced the electron density around the dye's anchoring unit, and thereby hindered orbital overlap between the LUMO

of the dye and the E_{CB} of the TiO_2 electrode.[54,55] Thus, dyes containing cyanoacrylic acid as their anchoring unit inject electrons more efficiently into the E_{CB} of the electrode and consequently produce higher photocurrent than dyes that have rhodanine acetic acid as the anchoring unit. When a strong electron-withdrawing group was placed around the anchoring unit of all-organic dyes, it also gave similar effect on the electron distribution (diminution of electron density near the anchoring groups).[33] As shown in Figure 8, the electron distributions of the LUMO state around on the anchoring units (cyanoacrylic acid) in PTD-03 and PTD-04 are spatially less dense than those in the PTD-02, because of the strong electron acceptors, benzo[*c*]-1,2,5-thiadiazole in PTD-03 and PTD-04. Instead, the electron density around the electron-withdrawing benzo[*c*]-1,2,5-thiadiazole looks to be strengthened, implying a less efficient electronic coupling between the dyes and the TiO_2.

Dye Design Regarding Dye Regeneration

Dye regeneration is one of the essential steps in converting absorbed light energy to electrical power in DSSCs. The driving force for dye regeneration in DSSCs is originated from the potential-energy difference between the oxidized dye's HOMO level and the redox potential of applied electrolyte in the DSSC. It has been reported that an insufficient driving force for dye regeneration causes a low open-circuit voltage (V_{oc}) and poor photocurrent generation, because of fast recombination between the injected electrons and the photooxidized dye molecules.[56] The photooxidized dye should also be regenerated rapidly to avoid charge recombination between the hole on the oxidized dye and the injected electron to the electrode and minimize chemical degradation during the DSSC operation cycle. Recently, the dye regeneration rate was measured by means of nanosecond transient absorption spectroscopy (TAS) with six different D–A-type all-organic dyes containing a carbazole moiety as a donor and cyanoacrylic acid as an acceptor.[14] The study showed that changes in structural parameters, such as conjugation length and the type of side chain, had minor effects on the dye regeneration efficiency if the potential difference between the dye and the electrolyte satisfies the minimum driving force of 20–25 kJ mol^{-1} ($\Delta E = 0.20$–0.25 V). Since the V_{oc} of the DSCC is limited by the difference between the E_{CB} of the semiconducting oxide electrode and the redox potential of the electrolyte, higher voltages can be theoretically achieved by using a redox shuttle with a higher redox potential. Further endeavors to optimize the efficiency of DSSCs should aim at matching a dye with the appropriate redox couple to yield a driving force of 20–25 kJ mol^{-1} for efficient dye regeneration. The energy levels of all-organic dyes are easily adjustable to the optimum by tuning conjugation length, chain conformation, and functional groups.

Dye Design Regarding Recombination

There are two different types of improper recombination in DSSCs. One is charge recombination between the semiconducting oxide electrode and the dye cation (inner-path recombination), which deteriorates electron-injection efficiency of organic dyes and leads to the decrease in photocurrent. The mechanism of the inner-path recombination is that the electron injected from a dye to the E_{CB} of an oxide electrode recombines again with the dye cation before the dye

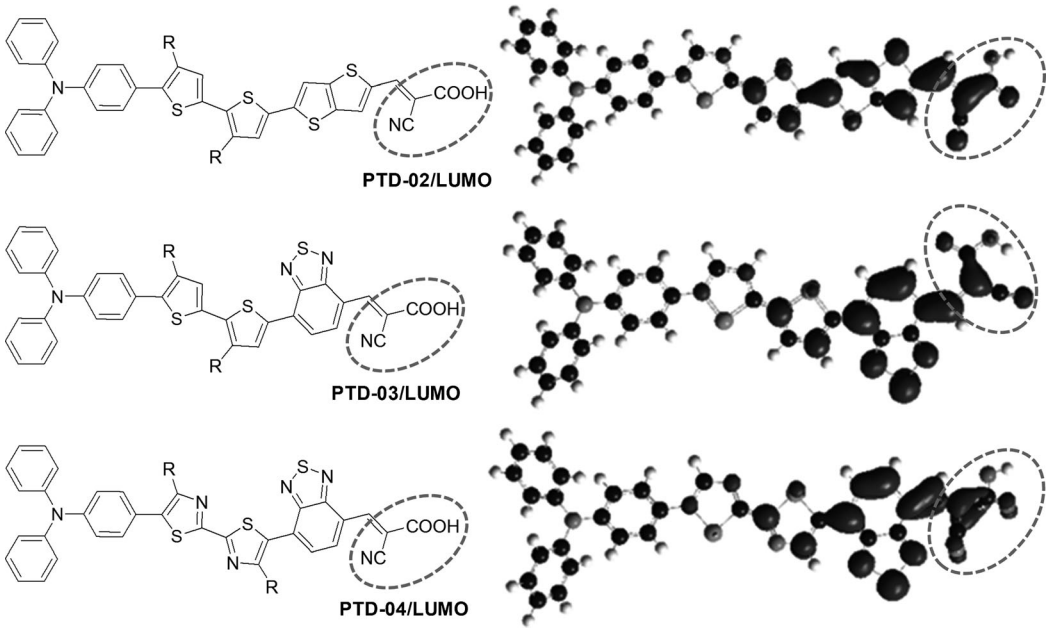

Figure 8. Electron locallization in LUMO state. The electron density near the anchoring unit decreases gradually when stronger electron-withdrawing groups are connected to the anchoring unit.

regeneration. The rate of inner recombination strongly depends on the molecular structure of the organic dyes and their arrangement on the surface of the oxide electrodes. The recombination rate can be determined by means of transient absorption spectroscopy by using two different laser spectrometers.[57] In the experiment, a dye-sensitized TiO_2 film is excited by a pulse laser in the absence of an electrolyte or while in contact with an inert electrolyte. Photon absorption by the dye results in electron injection into the TiO_2 film and a change of the electronic spectrum, indicating the formation of the dye cation. Recombination rate measurements are then carried out by monitoring the optical density change (ΔOD) at the wavelength at which the dye cation absorption is predominant. To prevent or retard this charge recombination, the produced positive charge density on all-organic dyes by the electron injection should be spatially separated from the oxide electrode. As depicted in Figures 7a and 8, most of electrons are localized around the electron-acceptor units in the excited D–A-type dyes, indicating that the positive-charge density would be dominant around the electron-donating moieties in the dye cation. As shown in Figure 4, inserting a π bridge into asymmetric D–A-type dyes facilitates charge transfer and subsequent charge separation between the donor and acceptor moieties in the excited state, which could effectively retard charge recombination. The spatial isolation of positive charge density from the oxide electrode is also largely determined by the dye's geometry and resulting arrangement on the surface. As depicted in Figure 9, the dye's orientation on the surface of TiO_2 is affected by the design of the anchoring units, although the rest of chemical nature of the applied dyes is essentially the same. Geometry optimization by means of computational calculations showed that the cyanoacrylic acid induces a vertically oriented dye geometry when it binds to TiO_2 surface, while the rhodanine acetic acid orients the dye with a tilt angle, resulting in a relatively shorter distance between the dye's donor moiety and the TiO_2 surface. Thus, dye cations with rhodanine acetic acid as an anchoring unit are prone to experience more inner-path recombination with the injected electrons.[53,54] Consequently, the selection of an anchoring unit of all-organic dyes could affect the electron-injection efficiency as well as the degree of inner-path recombination.

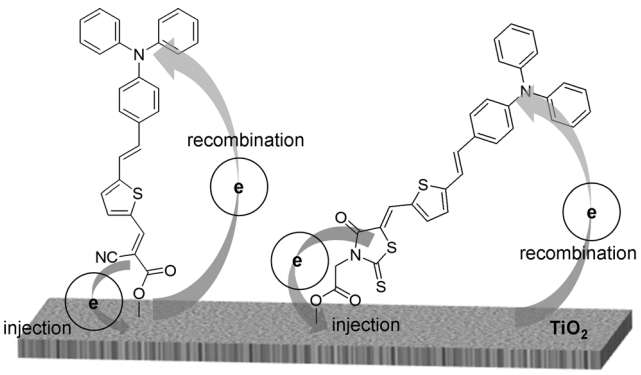

Figure 9. Anchoring units affect dye's orientation on the surface of TiO_2.

The other type of charge recombination in DSSCs occurs between the semiconducting oxide electrode and the electrolyte (outer-path recombination). This recombination decreases the theoretical potential difference between the oxide electrode and the electrolyte, resulting in a reduced V_{oc}. One of the common strategies to suppress this improper recombination path is preventing the electrolyte from approaching the surface of the semiconducting oxide electrode. Because most electrolytes in DSSCs are hydrophilic, inserting hydrophobic alkyl side chains or π bridges into the dye framework could inhibit the approach of the electrolytes to the oxide electrode surface. Densely packed hydrophobic all-organic dyes on the oxide electrode could passivate the electrode surface from the electrolytes, although the nature of the semiconducting oxide is hydrophilic. This strategy effectively suppresses charge recombination, resulting in enhanced V_{oc} values and an extended electron lifetime.[58,59] It has also been reported that introducing the star-burst triarylamine as a donor in a D–A-type dye provided a higher V_{oc} than similar dyes with a simple triarylamine donor. As illustrated in Figure 10, the dye containing a hydrophobic and extra-bulky triarylamine derivative as a donor group is superior in passivating the TiO_2 surface from the penetration of I_3^- of the electrolyte, which decreases charge recombination between TiO_2 and I_3^- and provides better device perform-

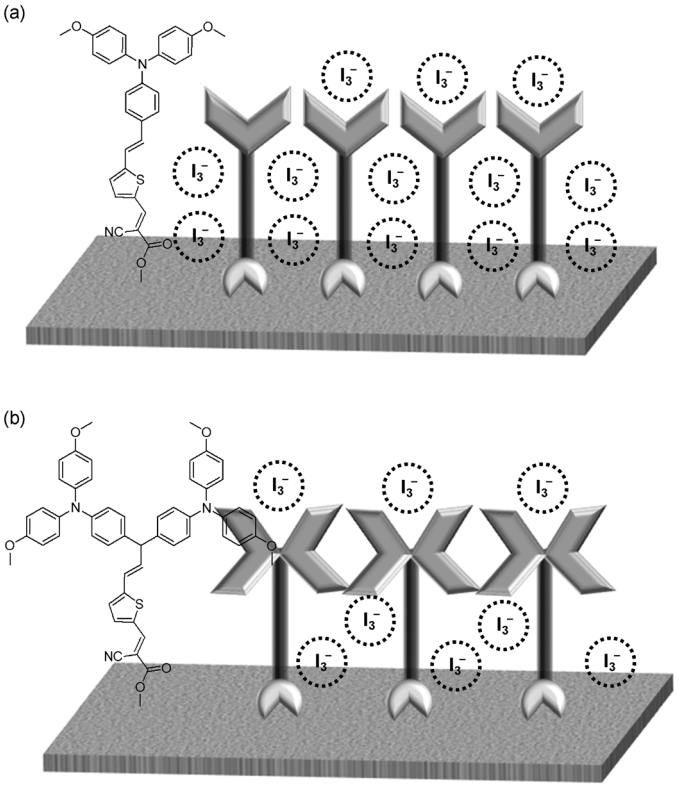

Figure 10. Extra-bulky triarylamine prevents the penetration of oxidized species of electrolyte.

ance including a higher V_{oc}.[60] However, one drawback of this dye design is that the sterically hindered dye structure reduces the number density of the adsorbed dyes on the oxide electrode surface, which decreases the absolute amount of injected electrons from the dyes to the electrode, resulting in poorer photocurrent generation in DSSCs.

In terms of a dye's compatibility with electrolytes, introducing 3,4-ethylenedioxythiophene (EDOT), methylidyne, and thiophene into the dye's conjugated frame could promote complexation between the dyes and the oxidized species (I_3^- and/or I_2) of the electrolyte, resulting in faster charge transport. This could be speculatively attributed to the electrostatic interactions as commonly seen in iodine doping of electron-donating organic species.[61] Specifically, inserting an EDOT unit into the middle of the π-bridge of all-organic dyes could facilitate the interaction between the dyes and I_2, because of the strong hydrophilic and electron-donating nature of EDOT. Computational calculations have also showed that all-organic dyes containing two EDOT units in their π bridge could make a stable complex with I_2 by means of the interactions between the oxygen atoms of EDOT and I_2.[62] However, the enhanced affinity toward electrolytes by the incorporation of a hydrophilic moiety into the all-organic dyes can also lower the V_{oc}, because their strong compatibility with hydrophilic electrolyte or Columbic interaction with oxidized electrolyte species can bring the oxidizing electrolyte species close to the electrode and promote the outer-path recombination.[63] Therefore, in the proper molecular design, a hydrophilic and electrolyte compatible moiety should be attached to the end or near the end of a D–A-type asymmetric dye, thereby promoting the charge transport by means of the redox chemistry throughout the electrolytes without enhancing the outer-path charge recombination.

Dye Design Regarding High V_{oc}

As discussed in the previous section, preventing improper charge recombination in DSSCs is one efficient strategy to obtain the theoretically achievable maximum V_{oc} under a given electrode/electrolyte system. Additionally, regulating the proper direction of interfacial dipole moment, which stems from dye's arrangement on the oxide electrode surface, is another way to enhance the V_{oc} in DSSCs. As shown in Figure 11, the actual E_{CB} of TiO_2 can be altered by the molecular dipole direction of the organic dyes at the interface of dye/TiO_2.[64,65] The dipole moment originates from electron localization within a dye molecule in the excited state. The magnitude and the direction of the interfacial dipole moment evenly influences the shift of the E_{CB} of the oxide electrode. The direction of the generated dipole in D–A-type organic dyes is generally from the electron-acceptor moiety to the donor moiety, because most electrons are localized around the electron-withdrawing unit in the excited state. Thus, D–A-type dyes containing an anchoring unit as an electron acceptor have the potential advantage to produce a proper direction of the dipole moment to provide a higher V_{oc} in DSSCs (Figure 11c). In addition, vertical orientation of D–A-type dye on the surface of the semiconducting oxide electrode would be important; it should be noted that rhodanine acetic acid as an anchoring unit in all-organic dyes induces a diagonal orientation of the dyes and produces mostly slanted dipole direction relative to the oxide electrode as we discussed in the previous section. A possible reason that most of the cationic organic dyes, such as merocyanine, hemicyanine, and cyanine derivatives, give a relatively low V_{oc} in DSSCs could also be due to the dipole moment effect. Because in the excited state electrons will reside on the cationic unit, cationic dyes generally have the opposite dipole direction relative to the conventional D–A-type dyes, inducing a downward shift of the E_{CB} of the oxide electrode and resulting in a reduced V_{oc} in DSSCs as shown in Figure 11b.

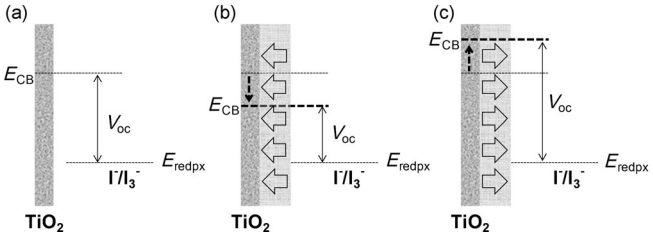

Figure 11. Interfacial dipole moment affects conduction band of TiO_2: a) without interfacial dipole moment, b) negative and c) positive dipole direction for V_{oc}.

Dye Design Regarding Long-Term Stability

For the practical application of DSSCs, long-term stability of the device having all-organic dyes must be at least comparable to the lifetime of inorganic semiconductor solar cells. There are several strategies, such as applying an ionic-liquid electrolyte or a solid hole-transporting agent in DSSCs, to improve the device stability of DSSCs. However, the most effective way is to devise chemically and photochemically robust dyes. All-organic dyes mostly consist of fully conjugated aromatic units that are vulnerable to oxidation. Particularly strong electron-donating moieties are more susceptible to chemical and photochemical degradation, as demonstrated by conjugated polymers that have such units.[66] Poly(3-hexylthiophene) and poly(*p*-phenyleneethynylene) exhibited noticeable damage to their emissive properties after acid or UV treatment with respect to polymers containing electron-withdrawing oxadiazole moieties. Nevertheless it has been demonstrated that under a specific operation condition of DSSCs, organic dyes composed of thiophene or perylene groups can provide enough stability for over 600 h as a sensitizer.[67,68] It has been also demonstrated that providing an additional electron-withdrawing unit and π-bridge between D–A-type organic dye frame (D–A-π-A) could improve stability.[45,46]

Although an applied organic dye is chemically stable, the desorption of the dye from the surface of the semiconducting oxide electrode is one of the critical problems leading to poor stability in DSSCs. All-organic dyes must have an anchoring unit to make a strong bond with the electrode. A carboxylic acid or its derivative is commonly adopted as the anchoring unit, because of its strong electronic coupling with the oxide electrode. A carboxyl group can form a bidentate bridge or chelating linkage with Brønsted acid sites on the TiO_2 surface, but the linkage can be easily hydrolyzed by water, causing instability of an operating DSSC. Recently, it has been reported that trialkoxysilane, $Si(OR)_3$, can form strong interactions with TiO_2 and provide negligible loss in the energy conversion efficiency under visible-light exposure for 600 h.[69] While this indicates that the trialkoxysilane is a promising anchoring group to improve the durability of DSSCs, the overall device performance is still not comparable to that of the devices adopting organic dyes with a carboxylic acid as an anchoring group, most likely due to the poor electron-withdrawing ability of trialkoxysilane as an acceptor in the D–A-type dyes.

Another approach to improve the long-term stability of organic dyes for DSSC applications is introducing hydrophobic side chains or aromatic rings around the donor unit of the D–A-type asymmetric dyes, which reduces dyes' water compatibility and as a consequence enhances the long-term stability as discussed in the outer-path recombination section. For example, when hydrophobic octyl or hexyl side chains were inserted into the π bridge in D–A-type all-organic dyes, the water-induced dye desorption phenomena were effectively suppressed and the initial DSSC performance was maintained over 600 h under a light irradiation.[70]

Summary and Outlook

In this contribution, we discuss molecular design concepts of all-organic dyes for DSSC application. Overall device performance of DSSCs is governed by the absorption, electron injection, and charge collection efficiencies. To maximize light harvesting of organic dyes, their absorption should be tailored to match with the high photon-flux region of solar radiation. The D–A-type dye design is one of promising strategies to achieve a desirable absorption region, because of the ICT-assisted absorption modulation. To improve the electron-injection efficiency, the anchoring unit of an all-organic dye should be able to undergo strong electronic coupling with the semiconducting oxide electrode. In addition the exciton binding energy of the dye should be minimized by rational molecular design. Since improper charge recombination deteriorates the overall light-to-electric-energy conversion efficiency, regulating the dye's assembly and orientation onto the electrode surface is essential in order to suppress such recombination. For example, the choice of the anchoring group will determine the principal orientation of the dyes, which will define the inner-path charge recombination distance and rate. Introducing hydrophobic moieties or at least excluding hydrophilic moieties near the anchoring unit effectively excludes the oxidized electrolytes from the electrode surface, and thereby reducing the outer-path recombination and rendering better device performance. The chemical and environmental stability of all-organic dyes is one of the key issues to sustain long-term operation of DSSCs, and it can be substantially ameliorated by structural modification of organic dyes.

Accumulated understanding about the effects of the structural modification of all-organic dyes on their photophysical and electrochemical behaviors has recently made considerable contribution to the device performance enhancement of DSSCs. Accordingly, the unlimited structural modification possibility and molecular arrangement give all-organic dyes a great potential to be an efficient sensitizer in DSSCs. The efficient energy-level modulation of organic dyes allows optimization of V_{oc} through matching the redox potential of a given or new electrolyte. The degree of solar-light harvesting, one of the critical issues inhibiting the improvement in device performance, can be optimized by separating the role of an anchoring unit and an electron-acceptor unit in the D–A-type organic dye design. While the anchoring unit enhances electronic coupling with the semiconducting oxide electrode, the electron-withdrawing group can induce strong ICT to redshift the dye's maximum absorption. Proper molecular design of all-organic dyes will continue to improve the solar-light-to-electric-energy conversion efficiency.

Acknowledgements

This work was supported by US Department of Energy (DoE), Office of Basic Science, as part of the Center for Solar and Thermal Energy Conversion, and Energy Frontier Research Center (DE-SC0000957).

[1] B. O'Regan, M. Grätzel, *Nature* **1991**, *353*, 737.
[2] N. Koumura, Z. S. Wang, S. Mori, M. Miyashita, E. Suzuki, K. Hara, *J. Am. Chem. Soc.* **2006**, *128*, 14256.
[3] F. Gao, Y. Wang, D. Shi, J. Zhang, M. Wang, X. Jing, R. Humphry-Baker, P. Wang, S. M. Zakeeruddin, M. Grätzel, *J. Am. Chem. Soc.* **2008**, *130*, 10720.
[4] A. Nattestad, A. J. Mozer, M. K. R. Fischer, Y. B. Cheng, A. Mishra, P. Bäuerle, U. Bach, *Nat. Mater.* **2010**, *9*, 31.
[5] J. N. Clifford, E. Martinez-Ferrero, A. Viterisi, E. Palomares, *Chem. Soc. Rev.* **2011**, *40*, 1635.
[6] T. Bessho, S. M. Zakeeruddin, C. Y. Yeh, E. W. G. Diau, M. Grätzel, *Angew. Chem.* **2010**, *122*, 6796; *Angew. Chem. Int. Ed.* **2010**, *49*, 6646.
[7] H. Wang, X. Zhang, F. Gong, G. Zhou, Z. S. Wang, *Adv. Mater.* **2012**, *24*, 121.
[8] M. Kimura, H. Nomoto, N. Masaki, S. Mori, *Angew. Chem.* **2012**, *124*, 4447.
[9] K. L. Wu, C. H. Li, Y. Chi, J. N. Clifford, L. Cabau, E. Palomares, Y. M. Cheng, H. A. Pan, P. T. Chou, *J. Am. Chem. Soc.* **2012**, *134*, 7488.
[10] M. Grätzel, *Acc. Chem. Res.* **2009**, *42*, 1788.
[11] A. Yella, H.-W. Lee, H. N. Tsao, C. Yi, A. K. Chandiran, Md. K. Nazeeruddin, E. W.-G. Diau, C.-Y. Yeh, S. M. Zakeeruddin, M. Grätzel, *Science* **2011**, *334*, 629.
[12] M. D. McGehee, *Science* **2011**, *334*, 607.

[13] P. Wang, S. M. Zakeeruddin, J. E. Moser, M. K. Nazeeruddin, T. Sekiguchi, M. Grätzel, *Nat. Mater.* **2003**, *2*, 402.
[14] T. Daeneke, A. J. Mozer, Y. Uemura, S. Makuta, M. Fekete, Y. Tachibana, N. Koumura, U. Bach, L. Spiccia, *J. Am. Chem. Soc.* **2012**, *134*, 16925.
[15] A. Hagfeldt, G. Boschloo, L. Sun, L. Kloo, H. Pettersson, *Chem. Rev.* **2010**, *110*, 6595.
[16] K. Norland, A. Ames, *Photogr. Sci. Eng.* **1970**, *14*, 295.
[17] C. Reich, W. D. Pandolfe, G. R. Bird, *Photogr. Sci. Eng.* **1973**, *17*, 334.
[18] W. Zeng, Y. Cao, Y. Bai, Y. Wang, Y. Shi, M. Zhang, F. Wang, C. Pan, P. Wang, *Chem. Mater.* **2010**, *22*, 1915.
[19] M. Xu, S. Wenger, H. Bala, D. Shi, R. Li, Y. Zhou, S. M. Zakeeruddin, M. Grätzel, P. Wang, *J. Phys. Chem. C* **2009**, *113*, 2966.
[20] K. Hara, T. Sato, R. Katoh, A. Furube, Y. Ohga, A. Shinpo, S. Suga, K. Sayama, H. Sugihara, H. Arakawa, *J. Phys. Chem. B* **2003**, *107*, 597.
[21] H. Tian, X. Yang, R. Chen, R. Zhang, A. Hagfeldt, L. Sun, *J. Phys. Chem. C* **2008**, *112*, 11023.
[22] M. Liang, W. Xu, F. Cai, P. Chen, B. Peng, J. Chen, Z. Li, *J. Phys. Chem. C* **2007**, *111*, 4465.
[23] K. Hara, Z. S. Wang, T. Sato, A. Furube, R. Katoh, H. Sugihara, Y. Dan-oh, C. Kasada, A. Shinpo, S. Suga, *J. Phys. Chem. B* **2005**, *109*, 15476.
[24] Z.-S. Wang, Y. Cui, K. Hara, Y. Dan-oh, C. Kasada, A. Shinpo, *Adv. Mater.* **2007**, *19*, 1138.
[25] K. Sayama, K. Hara, N. Mori, M. Satsuki, S. Suga, S. Tsukagoshi, Y. Abe, H. Sugihara, H. Arakawa, *Chem. Commun.* **2000**, 1173.
[26] M. O. Lenz, J. Wachtveitl, *J. Phys. Chem. C* **2008**, *112*, 11973.
[27] T. Horiuchi, H. Miura, K. Sumioka, S. Uchida, *J. Am. Chem. Soc.* **2004**, *126*, 12218.
[28] S. Ito, S. M. Zakeeruddin, R. Humphry-Baker, P. Liska, R. Charvet, P. Comte, M. K. Nazeeruddin, P. Péchy, M. Takata, H. Miura, S. Uchida, M. Grätzel, *Adv. Mater.* **2006**, *18*, 1202.
[29] H. Choi, C. Baik, S. O. Kang, J. Ko, M.-S. Kang, M. K. Nazeeruddin, M. Grätzel, *Angew. Chem.* **2008**, *120*, 333; *Angew. Chem. Int. Ed.* **2008**, *47*, 327.
[30] C.-H. Chen, Y.-C. Hsu, H.-H. Chou, K. R. J. Thomas, J. T. Lin, C.-P. Hsu, *Chem. Eur. J.* **2010**, *16*, 3184.
[31] K. Hara, Z.-S. Wang, Y. Cui, A. Furube, N. Koumura, *Energy Environ. Sci.* **2009**, *2*, 1109.
[32] Z.-S. Wang, N. Koumura, Y. Cui, M. Takahashi, H. Sekiguchi, A. Mori, T. Kubo, A. Furube, K. Hara, *Chem. Mater.* **2008**, *20*, 3993.
[33] B. G. Kim, C. G. Zhen, E. J. Jeong, J. Kieffer, J. Kim, *Adv. Funct. Mater.* **2012**, *22*, 1606.
[34] S. Hwang, J. H. Lee, C. Park, H. Lee, C. Kim, C. Park, M.-H. Lee, W. Lee, J. Park, K. Kim, N.-G. Park, C. Kim, *Chem. Commun.* **2007**, 4887.
[35] O. Kohle, M. Grätzel, A. F. Meyer, T. B. Meyer, *Adv. Mater.* **1997**, *9*, 904.
[36] D. Liu, R. W. Fessenden, G. L. Hug, P. V. Kamat, *J. Phys. Chem. B* **1997**, *101*, 2583.
[37] N. Kleinhenz, L. Yang, H. Zhou, S. C. Price, W. You, *Macromolecules* **2011**, *44*, 872. <
[38] J. R. Mann, M. K. Gannon, T. C. Fitzgibbons, M. R. Detty, D. F. J. Watson, *J. Phys. Chem. C* **2008**, *112*, 13057.
[39] S. Ito, H. Miura, S. Uchida, M. Takata, K. Sumioka, P. Liska, P. Comte, P. Pechy, M. Grätzel, *Chem. Commun.* **2008**, 5194.
[40] R. Chen, X. Yang, H. Tian, X. Wang, A. Hagfeldt, L. Sun, *Chem. Mater.* **2007**, *19*, 4007.
[41] M. K. Nazeeruddin, R. Humphry-Baker, P. Liska, M. Grätzel, *J. Phys. Chem. B* **2003**, *107*, 8981.
[42] S.-T. Huang, Y.-C. Hsu, Y.-S. Yen, H. H. Chou, J. T. Lin, C.-W. Chang, C.-P. Hsu, C. Tsai, D.-J. Yin, *J. Phys. Chem. C* **2008**, *112*, 19739.
[43] S. Haid, M. Marszalek, A. Mishra, M. Wielopolski, J. Teuscher, J. E. Moser, R. Humphry-Baker, S. M. Zakeeruddin, M. Grätzel, P. Bäuerle, *Adv. Funct. Mater.* **2012**, *22*, 1291.
[44] Y. Wu, M. Marszalek, S. M. Zakeeruddin, Q. Zhang, H. Tian, M. Grätzel, W. Zhu, *Energy Environ. Sci.* **2012**, *5*, 8261.
[45] Y. Wu, W. Zhu, *Chem. Soc. Rev.* **2013**, *42*, 2039.
[46] K. Pei, Y. Wu, W. Wu, Q. Zhang, B. Chen, H. Tian, W. Zhu, *Chem. Eur. J.* **2012**, *18*, 8190.
[47] B. K. An, S. K. Kwon, S. D. Jung, S. Y. Park, *J. Am. Chem. Soc.* **2002**, *124*, 14410.
[48] W. Zhu, Y. Wu, S. Wang, W. Li, X. Li, J. Chen, Z. Wang, H. Tian, *Adv. Funct. Mater.* **2011**, *21*, 756.
[49] Y. Ooyama, A. Ishii, Y. Kagawa, I. Imae, Y. Harima, *New J. Chem.* **2007**, *31*, 2076.
[50] Y. Chen, Z. Zeng, C. Li, W. Wang, X. Wang, B. Zhang, *New J. Chem.* **2005**, *29*, 773.
[51] M. Knupfer, *Appl. Phys. A* **2003**, *77*, 623.
[52] R. A. Marcus, N. Sutin, *Biochim. Biophys. Acta Rev. Bioenerg.* **1985**, *811*, 265.
[53] H. Tian, X. Yang, R. Chen, Y. Pan, L. Li, A. Hagfeldt, L. Sun, *Chem. Commun.* **2007**, 3741.
[54] J. Wiberg, T. Marinado, D. P. Hagberg, L. Sun, A. Hagfeldt, B. Albinsson, *J. Phys. Chem. C* **2009**, *113*, 3881.
[55] X. Huanga, Y. Fangb, X. Lia, Y. Xiea, W. Zhu, *Dyes Pigm.* **2011**, *90*, 297.
[56] T. Daeneke, A. J. Mozer, T. H. Kwon, N. W. Duffy, A. B. Holmes, U. Bach, L. Spiccia, *Energy Environ. Sci.* **2012**, *5*, 7090.
[57] X. H. Zhang, Y. Cui, R. Katoh, N. Koumura, K. Hara, *J. Phys. Chem. C* **2010**, *114*, 18283.
[58] Z. Ning, H. Tian, *Chem. Commun.* **2009**, 5483.
[59] S.-H. Lin, Y.-C. Hsu, J. T. Lin, C.-K. Lin, J.-S. Yang, *J. Org. Chem.* **2010**, *75*, 7877.
[60] J. Tang, J. Hua, W. Wu, J. Li, Z. Jin, Y. Long, H. Tian, *Energy Environ. Sci.* **2010**, *3*, 1736.
[61] K. Tashiro, M. Kobayashi, T. Kawai, K. Yoshino, *Polymer* **1997**, *38*, 2867.
[62] M. Planells, L. Pellejá, J. N. Clifford, M. Pastore, F. D. Angelis, N. López, S. R. Marder, E. Palomares, *Energy Environ. Sci.* **2011**, *4*, 1820.
[63] Y. Liang, F. Cheng, J. Liang, J. Cheni, *J. Phys. Chem. C* **2010**, *114*, 15842.
[64] Y. Jiao, F. Zhang, M. Grätzel, S. Meng, *Adv. Funct. Mater.* **2013**, *23*, 424.
[65] P. Chen, J. H. Yum, F. D. Angelis, E. Mosconi, S. Fantacci, S. J. Moon, R. H. Baker, J. Ko, M. K. Nazeeruddin, M. Grätzel, *Nano Lett.* **2009**, *9*, 2487.
[66] K. Lee, H. J. Kim, J. C. Cho, J. Kim, *Macromolecules* **2007**, *40*, 6457.
[67] T. Edvinsson, C. Li, N. Pschirer, J. Schöneboom, F. Eickemeyer, R. Sens, G. Boschloo, A. Herrmann, K. Müllen, A. Hagfeldt, *J. Phys. Chem. C* **2007**, *111*, 15137.
[68] J.-J. Kim, H. Choi, J.-W. Lee, M.-S. Kang, K. Song, S. O. Kang, J. Ko, *J. Mater. Chem.* **2008**, *18*, 5223.
[69] C. Baik, D. Kim, M.-S. Kang, S. O. Kang, J. Ko, M. K. Nazeeruddin, M. Grätzel, *J. Photochem. Photobiol. A* **2009**, *201*, 168.
[70] X.-H. Zhang, Z.-S. Wang, Y. Cui, N. Koumura, A. Furube, K. Hara, *J. Phys. Chem. C* **2009**, *113*, 13409.

Received: December 5, 2012
Published online: March 11, 2013

